ARTICLE IN PRESS

BMB Reports - Manuscript Submission

Manuscript Draft

DOI: 10.5483/BMBRep.2022-0139

Manuscript Number: BMB-22-139

Title: Particulate matter induces ferroptosis by accumulating iron and dysregulating the antioxidant system

Article Type: Article

Keywords: Particulate matter; Cell death; Ferroptosis; iron accumulation; ROS

Corresponding Author: Seon-Jin Lee

Authors: Minkyung Park[1,2], Young-Lai Cho[1], Yumin Choi[1,2], Jeong-Ki Min[3], Young-Jun Park[1,2], Sung-Jin Yoon[1,2], Dae-Soo Kim[1,2], Mi-Young Son[1,2], Su Wol Chung[4], Heedoo Lee[5], Seon-Jin Lee[1,2,*]

Institution: [1]Environmental Disease Research Center, Korea Research Institute of Bioscience and Biotechnology,
[2]Department of Functional Genomics, University of Science and Technology (UST),
[3]MabTics, Co. Ltd,
[4]School of Biological Sciences, University of Ulsan,
[5]Department of Biology and Chemistry, Changwon National University,

UNCORRECTED PROOF

ARTICLE IN PRESS

Manuscript Type: Article

Field under which paper is to be reviewed: Biomedical Science

Title: Particulate matter induces ferroptosis by accumulating iron and dysregulating the antioxidant system.

Authors: Minkyung Park[a,b], Young-Lai Cho[a], Yumin Choi[a,b], Jeong-Ki Min[c], Young-Jun Park[a,b], Sung-Jin Yoon[a,b], Dae-Soo Kim[a,b], Mi-Young Son[a,b], Su Wol Chung[d], Heedoo Lee[e*] and Seon-Jin Lee [a,b*]

Affiliation:

[a] Environmental Disease Research Center, Korea Research Institute of Bioscience and Biotechnology (KRIBB), Daejeon, 34141, Korea

[b] Department of Functional Genomics, University of Science and Technology (UST), Daejeon, 34113, Korea

[c] MabTics Co. Ltd, Daejeon, 34141, Korea

[d] School of Biological Sciences, University of Ulsan, Ulsan, 44610, Korea

[e] Department of Biology and Chemistry, Changwon National University, Changwon, 51140, Korea

Running Title: Particulate matter increases ferroptosis.

Corresponding Author: Seon-Jin Lee, Ph.D., Environmental Disease Research Center, Korea Research Institute of Bioscience and Biotechnology, Daejeon 34141, South Korea. Tel: +82-42-879-8293; E-mail: sjlee@kribb.re.kr; Heedoo Lee, Ph.D., Department of Biology and Chemistry, Changwon National University, Changwon, 51140, South Korea. Tel: +82-55-213-3452; E-mail: leehd@changwon.ac.kr

UNCORRECTED PROOF

ABSTRACT

Particulate matter is an air pollutant composed of various components that has adverse effects on the human body. Particulate matter is known to induce cell death by generating an imbalance in the antioxidant system; however, the underlying mechanism has not been elucidated. In the present study, we demonstrated the cytotoxic effects of the size and composition of particulate matter on small intestine cells. We found that particulate matter 2.5 ($PM_{2.5}$) with extraction ion (EI) components ($PM_{2.5}$ EI), is more cytotoxic than PM containing only polycyclic aromatic hydrocarbons (PAHs). Additionally, PM-induced cell death is characteristic of ferroptosis and includes iron accumulation, lipid peroxidation, and reactive oxygen species (ROS) generation. Furthermore, ferroptosis inhibitor as liprostatin-1 and iron-chelator as deferiprone attenuated cell mortality, lipid peroxidation, iron accumulation, ROS production after $PM_{2.5}$ EI treatment in human small intestinal cells. These results suggest that $PM_{2.5}$ EI may increase ferroptotic-cell death by iron accumulation and ROS generation and be a potential therapeutic clue for inflammatory bowel diseases in human small intestinal cells.

Keywords: Particulate matter, cell death, ferroptosis, iron accumulation, ROS

UNCORRECTED PROOF

INTRODUCTION

Particulate matter (PM) is a global concern that has a significant effect on human (1). Particle diameter is widely used to subdivide PM into PM_{10} and $PM_{2.5}$, and contains metal ions, sulfates, ammonium nitrate, proteins, and organic materials, including polycyclic aromatic hydrocarbons (PAHs) (2). Exposure to PM induces many adverse consequences, including cardiovascular and respiratory diseases. Following PM inhalation, some PM may translocate to the gastrointestinal tract and contribute to gastrointestinal diseases (3,4).

Previous studies have reported a relationship between PM and several types of cell death (5). Specifically, PM exposure demonstrably induces oxidative stress resulting in increased reactive oxygen species (ROS) that are key factors in cellular responses under normal physiological conditions and are regulated by antioxidant enzymes (6,7). However, excessive ROS production can induce lipid peroxidation, which has adverse effects on cells, leading to various types of cell death, including apoptosis, autophagy, and ferroptosis (7).

Ferroptosis is defined as non-apoptotic programmed cell death characterized by iron-induced ROS accumulation and lipid peroxidation (8). Ferroptosis is morphologically and functionally distinct from apoptosis (8). A key enzyme in ferroptosis, GPX4, converts reduced glutathione to oxidized glutathione and functions as an antioxidant enzyme (9). System Xc^- (xCT) is also important in ferroptosis and functions by exchanging extracellular cystine with intracellular glutamate (9). Therefore, xCT regulates the cysteine/glutathione ratio and protects cells against oxidative damage (9). When these enzymes lose their functions, redox homeostasis is disrupted and ferroptosis is induced. Furthermore, ROS are equally essential in the induction of ferroptosis (10). Abnormal oxygen reduction results in ROS, including peroxide anions, hydrogen peroxide (H_2O_2), and hydroxyl radicals (10). Iron accumulation is central to ferroptosis (10). When ferric iron (Fe^{3+}) is imported into the cytoplasm, it is reduced to ferrous

UNCORRECTED PROOF

iron (Fe^{2+}) (10). Excessive iron induces the Fenton reaction that produces ROS and lipid peroxides, which are able to induce ferroptosis. Numerous studies demonstrated that PM increases cellular ROS, iron accumulation, and lipid peroxidation and induces ferroptosis in the gastrointestinal tract (6, 11). However, the underlying mechanisms of PM-induced programmed cell death, particularly ferroptosis, remain unknown.

In this study, human small intestinal cells were used to investigate PM-induced cell death. We demonstrated that $PM_{2.5}$ with extraction ions (EI) had the most cytotoxic effect and induced ferroptosis. Furthermore, the results suggest that components of PM, namely EI, are critical to the induction of intestinal diseases and cell death, including apoptosis, necrosis, and ferroptosis.

RESULTS

Cytotoxicity of $PM_{2.5}$ with extraction ions is greater than that of PM with PAHs.

The cytotoxicity on human small intestinal cell lines (HuTu-80) were determined for three types of PM, including PM_{10} and $PM_{2.5}$, containing PAHs, and $PM_{2.5}$, containing EIs. Treatment with PM_{10} or $PM_{2.5}$ PAHs of varying concentrations (1, 10, 25, 50, 100, and 200 μg/mL) had no significant effect on HuTu-80 cell viability after 24 h. However, the viability of $PM_{2.5}$ EI-exposed cells decreased in a dose-dependent manner (Fig. 1A). Additionally, HuTu-80 cells were exposed to 100 μg/mL of the three types of PM for 24, 48, and 72 h, after which cell viability was measured using the crystal violet assay. Cell viability decreased in a time-dependent manner, and $PM_{2.5}$ EI showed the greatest decrease in viability (Fig. 1B). To detect the level of apoptosis, the toxicity of the three PM types following HuTu-80 cell exposure was evaluated using a Dead Cell Apoptosis Kit, the Annexin V with fluorescein isothiocyanate (FITC) and propidium iodide (PI) (Fig. 1C) in addition to Hoechst 33342 staining (Fig. 1D). As expected, PM induced apoptotic cell death, and apoptotic cell death caused by $PM_{2.5}$ EI was

UNCORRECTED PROOF

the greatest. Taken together, $PM_{2.5}$ EI had more cytotoxic effects than PM_{10} PAHs or $PM_{2.5}$ PAHs.

Ferroptotic and apoptotic cell death induced by $PM_{2.5}$ EI.

Western blot analysis of HuTu-80 cells stimulated with 25 μg/mL PM for 24 h demonstrated that treatment with PM significantly upregulated apoptosis-related proteins and HO-1 (Fig. 2A, 2B), and downregulated key ferroptosis regulators, GPX-4 and xCT (Fig. 2B). Furthermore, these results demonstrated that $PM_{2.5}$ EI had the highest apoptotic and ferroptotic cell death level, as expected. To confirm this, HuTu-80 cells were treated with the lipid peroxidation inhibitor liproxstatin-1 (Lip-1), iron chelator deferiprone (DFP), and inhibitors of apoptosis, benzyloxycarbonyl-Val-Ala-Asp-fluoromethyl ketone Z-VAD-fmk in the presence of $PM_{2.5}$ EI. The cell viability assay revealed that the decreased levels of cell viability resulting from $PM_{2.5}$ EI were inhibited by Lip-1, DFP, and Z-VAD-fmk (Fig. 2C, 2E). We also demonstrated that $PM_{2.5}$ EI were increased in the ferroptosis and apoptosis levels by western blot analysis and inhibited ferroptosis and apoptosis from the inhibitor of Lip-1, DFP, and Z-VAD-fmk in translational levels (Fig. 2D, 2F). No significant difference was identified between cell viability or protein levels of autophagy or necrosis inhibitors (chloroquine and necrosufonamide) and $PM_{2.5}$ EI. Thus, $PM_{2.5}$ EI could be modulated by ferroptosis and apoptosis rather than autophagy and necrosis.

Ferroptosis by lipid peroxidation and iron accumulation induced by $PM_{2.5}$ EI.

As lipid peroxidation and iron accumulation are critical events of ferroptotic cell death (8), we determined if PM induces lipid peroxidation and whether ferroptosis inhibitors would suppress lipid peroxidation resulting in PM-exposed HuTu-80 cells. Malondialdehyde (MDA) is one of

UNCORRECTED PROOF

the end products of lipid peroxides, so MDA levels are used as a marker of lipid peroxidation (10). MDA levels with PM treatment increased in a dose-dependent manner, and $PM_{2.5}$ EI generated more MDA than PM PAHs (Fig. 3A). Similar to these results, the levels of total iron increased in a dose-dependent manner, and treatment with $PM_{2.5}$ EI demonstrated the greatest efficiency in inducing increased iron levels (Fig. 3C). As these results indicate an increase in ferroptosis, the levels of MDA and total iron during the treatment of ferroptosis inhibitors with PM were examined. The results demonstrated that the increased levels of both MDA and total iron by PM were reduced by ferroptosis inhibitors (Fig. 3B, D). Additionally, the expression levels of iron-related proteins were investigated. The degradation of iron protein complexes, ferritin, or the increase of the iron transporter, transferrin receptor, result in increased intracellular levels of iron (11). The translational levels of ferritin and transferrin receptors were regulated to induce ferroptosis in response to $PM_{2.5}$ EI, but no significant effect was observed in response to PM PAHs (Fig. 3E). In addition, transferrin had no significant effect on PM with PAHs or EI (Fig. 3E). Ferroptosis induced by $PM_{2.5}$ EI is therefore associated with iron homeostasis and is regulated by iron-related proteins.

Increased ROS generation due to $PM_{2.5}$ EI leads to ferroptosis.

Intracellular ROS is generated as a result of PM and ROS is related to ferroptosis (6). We investigated ROS levels following treatment with the three types of PM. As expected, ROS levels following $PM_{2.5}$ EI treatment increased in a dose-dependent manner; however, PM PAHs had no significant effect on ROS levels (Fig. 4A). N-acetylcysteine (NAC), a known ROS scavenger, is a precursor of the antioxidant glutathione, which is related to ferroptosis. Mito-TEMPO, a mitochondrial superoxide scavenger, and diphenyleneiodonium chloride (DPI), an NADPH-oxidase inhibitor, also block intracellular ROS generation. To investigate whether

UNCORRECTED PROOF

$PM_{2.5}$ EI-induced ROS production was involved in $PM_{2.5}$ EI-induced cell death, we examined the effect of ROS inhibitors with $PM_{2.5}$ EI treatment. The cell viability assay demonstrated that both NAC and mito-TEMPO significantly increased cell viability, but did not significantly affect DPI treatment (Fig. 4B). Also, treatment with NAC or mito-TEMPO recovered the initial ROS levels that were increased by $PM_{2.5}$ EI in HuTu-80 cells (Fig. 4C). The ROS are related to antioxidant enzymes, such as superoxide dismutases (SODs), which convert superoxide anions to H_2O_2; therefore, these enzymes can suppress ferroptosis (10). Western blot analysis demonstrated that the translational levels of SODs decreased following treatment with $PM_{2.5}$ EI for 24 h (Fig. 4D). To further investigate whether $PM_{2.5}$ EI-induced ROS production is related to ferroptosis, $PM_{2.5}$ EI was treated with Lip-1. ROS levels were recovered by Lip-1 (Fig. 4E), and SOD expression levels were upregulated by lipid peroxidation inhibitor and iron chelator (Fig. 4F). Furthermore, the expression levels of iron-related proteins, ferritin and transferrin receptor were downregulated the activity of ferroptosis after treatment with ferroptosis inhibitors (Fig. 4G). Therefore $PM_{2.5}$ EI-induced ROS production may cause ferroptosis in intestinal cells.

DISCUSSION

The composition of PM includes several components, such as organic materials, including PAHs, several metal ions, sulfates, ammonium nitrate, and protein complexes (2). In the gastrointestinal tract, PM is known to induce several types of programmed cell death (7, 11); however, the specific components and underlying mechanisms that induce cell death have not yet been elucidated. In this study, we determined that PM induces several types of cell death, and our results indicate that PM EI is the main culprit in the regulation of cell death (7). Ferroptosis is characterized by iron accumulation, lipid peroxidation, and increased ROS levels,

UNCORRECTED PROOF

so inhibition of these suppresses ferroptosis (8, 12). Here, we report that $PM_{2.5}$ EI induces ferroptotic cell death, which is inhibited by the prevention of iron accumulation, lipid peroxidation, and ROS generation. Thus, our results validate our hypothesis that the PM EI has a more detrimental effect on health than PM PAHs.

Iron is a key element in numerous biological functions and metabolic processes in humans. Therefore, the maintenance of iron homeostasis is crucial. Iron homeostasis is mediated by balancing intracellular iron levels through the regulation of iron uptake, storage, and utilization. This system is tightly regulated by several proteins (11). In brief, iron binds to transferrin, the complex then binds to its receptor, the transferrin receptor on the cell membrane, and is then imported to the intracellular surface (11). Excess intracellular iron is stored in ferritin (11). A previous study reported that $PM_{2.5}$ can destroy iron intake and storage and downregulate several ferroptosis enzymes (13). Consistent with this, we established that exposure to $PM_{2.5}$ increased the total iron levels and altered the expression of iron-related proteins. Iron levels also increased with PM PAHs, but even more with $PM_{2.5}$ EI. Since the $PM_{2.5}$ EI used in the experiment contains some metal ions and irons, we speculated that ferroptosis is induced by increased intracellular iron levels while PM EI is taken up by the cell rather than PM PAHs. The intracellular iron-containing protein ferritin is downregulated by $PM_{2.5}$ EI exposure, and the carrier protein for the transferrin-iron complex and transferrin receptor are upregulated by $PM_{2.5}$ EI. These were recovered by ferroptosis inhibitors. Furthermore, several key enzymes of ferroptosis, GPX4 and xCT were downregulated during $PM_{2.5}$ EI exposure and it was recovered by ferroptosis inhibitors. These enzymes directly or indirectly regulate glutathione (GSH) which is important for the elimination of lipid peroxides, so they serve to protect cells against ferroptosis induced by excessive iron levels (9). Taken together, our results demonstrate that the increased intracellular iron levels following $PM_{2.5}$ EI treatment regulate protein expression

UNCORRECTED PROOF

and induce ferroptosis by lipid peroxidation.

The reduction of oxygen forms ROS that have high reaction power. ROS are categorized as mitochondrial ROS and NADPH-related ROS. Antioxidants attenuate the adverse effects of ROS. The reduction in cell viability caused by $PM_{2.5}$ EI was restored by mito-TEMPO. Conversely, the NADPH-oxidase inhibitor DPI had no effect on cell viability, confirming that ROS production by PM is related to mitochondrial ROS.

Heme oxygenase-1 (HO-1) is the major intracellular source of iron and is an essential enzyme for iron-dependent lipid peroxidation during ferroptosis (14). Consistent with this report, we determined that exposure to $PM_{2.5}$ increased the levels of Nrf2 and HO-1, and its endogenous inhibitor, Kelch-like ECH-associated protein 1 (Keap1), was downregulated. Therefore, the upregulation of HO-1 may induce ferroptosis through lipid peroxidation and the generation of ROS by $PM_{2.5}$ EI.

Autophagy has a dual role to regulate cellular homeostasis or cell death, thus the functions of autophagy are controversial. On one hand, autophagy can protect cells from apoptosis by the responses to toxic molecules (15). On the other hand, $PM_{2.5}$ increased cell mortality by impairment of autophagic flux, not autophagic activity and it may promote apoptotic cell death (16). Our results demonstrated that inhibition of autophagic flux by increased p62 and decreased ATG5 levels for $PM_{2.5}$ EI treatment and impairment of autophagic flux. These results suggested that $PM_{2.5}$ EI might attenuate autophagic processes and autophagosome degradation by the inhibition of lysosomal protein such as LAMP-2.

In conclusion, we established that $PM_{2.5}$ EI plays an essential role in PM cytotoxicity in small intestinal cells. Furthermore, this cytotoxicity is due to iron accumulation, lipid peroxidation, and ROS generation caused by an imbalance in the antioxidant system, which ultimately induces ferroptosis. Therefore, our findings suggest that a mechanism for the treatment of PM-

UNCORRECTED PROOF

induced diseases may be helpful for a potential therapeutic clue for inflammatory bowel disease and Crohn's disease.

MATERIALS AND METHODS

Reagents and antibodies. Particulate matter (PM_{10} PAH, $PM_{2.5}$ PAH, and $PM_{2.5}$ EI) was purchased from European Reference Materials (ERM-CZ100, ERM-CZ110; B-2440 European Commission, Geel, Belgium). $PM_{2.5}$ PAHs were also obtained by separation from the PM_{10} certified reference material (i.e., ERM-CZ100) based on the modified sedimentation method (17). Liproxstatin-1 (SML1414), Deferiprone (379409), and Chloroquine (C6628) were purchased from Sigma-Aldrich Chemical Co. Inc. (St Louis, MO, USA). Necrosulfonamide (20844) and mito-TEMPO (16621) were purchased from Cayman Chemical Co. (Ann Arbor, MI, USA). Z-VAD-fmk (cs-0015633) was purchased from ChemScene (Monmouth Junction, NJ, USA). *N*-acetyl-L-cysteine (A0905) was purchased from Tokyo Chemical Industry Co., Ltd. (Chiyodaku, Tokyo, Japan). The following antibodies were used: HO-1 (ADI-SPA-816; Enzo Biochem Inc., NY, USA), xCT (NB300-318; Novus Biologicals, CO, USA), transferrin receptor (13-6800; Invitrogen, MA, USA), ferritin (ab75973) and transferrin (ab1223; Abcam, Cambridge, UK), LC3B (L7543), and p62 (P0067; Sigma-Aldrich Chemical Co. Inc., MO, USA). The proteins and inhibitors, β-actin (sc-47778), p53 (sc-6243), cleaved Caspase-9 (sc-56073), Keap1 (sc-33569), Nrf2 (sc-722), ATG5 (sc-133158), and ATG7 (sc-33211) were obtained. SOD1 (sc-11407), SOD2 (sc-30080), catalase (sc-50508; Santa Cruz Biotechnology Inc., CA, USA), cleaved Caspase-3 (9661s), cleaved PARP (5625s), and GPX-4 (52455s; Cell Signaling Technology Co., MA, USA).

UNCORRECTED PROOF

Cells and cell culture. The small intestine cell line HuTu-80 was cultured in Dulbecco's modified Eagle's medium (DMEM; SH30243.01; Hyclone, UT, USA) supplemented with 10% fetal bovine serum (SH30919.03; Hyclone, Logan, UT, USA) and 1X antibiotic–antimycotic (100 u/mL penicillin, 100 µg/mL streptomycin, and 0.25 µg/mL Fungizone®; LS 203-01; Welgene Inc., Gyeongsan, Korea) at 37°C in a humidified incubator with 5% carbon dioxide. Cells were then treated with the three types of PM in the presence or absence of various concentrations of cell death inhibitors.

Cell viability assay. Cell viability was measured using the WST-8 assay (QM10000; Biomax Institute, Seoul, Korea) and the crystal violet assay. HuTu-80 cells were plated on 96- or 12-well plates for 24 h. The cells were incubated with (or without) different concentrations of the three types of PM and various cell death inhibitors for 24 h. For the WST-8 assay, WST-8 was added to each well and incubated at 37°C in the dark. After incubation, absorbance was quantified at 450 nm using a SpectraMax ABS Plus microplate reader (Molecular Devices, San Jose, CA, USA). For the crystal violet assay, the plate was gently washed with phosphate buffered saline (PBS) and incubated for 1 min with crystal violet solution. After incubation, the samples were carefully washed several times with tap water and left to dry. The absorbance was quantified at 570 nm using a SpectraMax ABS Plus microplate reader (Molecular Devices, San Jose, CA, USA).

Quantification of apoptosis by flow cytometry. The degree of apoptosis was assessed using the Dead Cell Apoptosis Kit, Annexin V with fluorescein isothiocyanate and PI and flow cytometry (V13242, Invitrogen, MA, USA) in accordance with the manufacturer's instructions. The samples were analyzed using a NovoCyte Flow Cytometer.

UNCORRECTED PROOF

Hoechst 33342 staining. Apoptosis was detected using Hoechst 33342 solution (62249, Thermo Scientific, IL, USA). HuTu-80 cells were seeded on a confocal dish (211350, SPL, Pochon, South Korea) and treated with three types of PM (100 μg/mL). After 24 h, cells were washed with PBS and incubated with Hoechst 33342 solution (1 μg/mL) for 10 min at 37°C. Apoptosis was then detected using fluorescence microscopy.

Detection of MDA. Lipid peroxidation was detected by quantification of the MDA concentration in cell lysates using the Lipid Peroxidation (MDA) Assay Kit (ab118970, Abcam, Cambridge, UK) according to the manufacturer's protocol.

Measurement of iron accumulation. The levels of total iron were assessed by quantifying the iron concentration in cell lysates using a colorimetric Iron Assay Kit (ab83366, Abcam, Cambridge, UK) according to the manufacturer's protocol.

Detection of ROS generation. ROS formation in HuTu-80 cells was detected using a DCFDA/H2DCFDA-Cellular ROS Assay Kit (ab113851, Abcam, Cambridge, UK) according to the manufacturer's protocol.

Western blot analysis. The cells were lysed on ice using a radioimmunoprecipitation assay lysis buffer and 1X protease inhibitor cocktail (Sigma-Aldrich Chemical Co. Inc., MO, USA) for 30 min. Lysates were quantified using a Pierce® BCA Protein Assay Kit (Thermo Scientific, IL, USA) and separated on a 6–15% gel with sodium dodecyl sulfate-polyacrylamide gel electrophoresis and then transferred to a PVDF membrane using a Trans-Blot® Turbo™

UNCORRECTED PROOF

Transfer pack (Bio-Rad, CA, USA). The membranes were blocked with 5% skim milk/TBST for 1 h and incubated with primary antibodies overnight at 4°C. After three washes, the membranes were incubated with horseradish peroxidase (HRP)-conjugated secondary antibodies for 40 min at room temperature. After washing for 2 h, protein bands were visualized using Clarity Western ECL Substrate.

Statistical analysis. Quantitative data are represented as mean ± standard deviation, and significance was determined by performing a two-tailed, unpaired Student's *t*-test. Statistical significance was set at $p < 0.05$.

UNCORRECTED PROOF

ARTICLE IN PRESS

ACKNOWLEDGMENTS

This research was funded by the KIST Institutional Program (2E31700- 22-P005), the KRIBB Research Initiative Program (KGM5322113), and the national research foundation (NRF-2014R1A6A1030318 and NRF-2021R1A2C1094382).

CONFLICTS OF INTEREST

The authors declare no conflict of interest.

UNCORRECTED PROOF

FIGURE LEGENDS

Figure 1. $PM_{2.5}$ containing extractive ions cause apoptosis more strongly than PM containing PAHs. Cell viability analysis in response to treatment of three types of PM after 24 h using WST-8 (A) and three types of PM (100 μg/ml) after 24, 48, 72 h using crystal violet assay (B). Identification of cell death induced by PM (100 μg/mL) for 24 h with Annexin-V/ propidium iodide (PI) double staining assessed using flow cytometry (**C**) and Hoechst staining assessed using a fluorescence microscope (40x) (**D**). The experiment was repeated three times. *$p < 0.05$, #$p < 0.001$.

Figure 2. Ferroptosis induced by $PM_{2.5}$ EI due to ferroptosis-related protein expression regulation. (**A, B**) Western blot analysis after incubation of 25 μg/mL of three types of PM for 24 h. (**C, E, G**) Cell viability analysis after preincubation with Liproxstatin-1 (1 μM), Deferiprone (100 μM), Z-VAD-fmk (10 μM), Chloroquine (10 μM) or Necrosulfonamide (0.5 μM) for 2 h and subsequent stimulation with 25 μg/mL of $PM_{2.5}$ EI for 24 h using WST-8. (**D, F, H**) Western blot analysis after pretreatment with Liproxstatin-1 (1 μM), Deferiprone (100 μM), Z-VAD-fmk (10 μM), Chloroquine (10 μM) or Necrosulfonamide (0.5 μM) for 2 h and subsequent stimulation with 25 μg/mL of $PM_{2.5}$ EI for 24 h. The experiment was repeated three times. *$p < 0.05$, #$p < 0.001$.

Figure 3. The type of cell death induced by $PM_{2.5}$ with extraction ions is characteristic of ferroptosis. (**A**) Malondialdehyde (MDA) formation as a marker of lipid peroxidation in HuTu-80 cells incubated with three types of PM after 12 h using a lipid peroxidation assay kit. (**B**) Detection of MDA in HuTu-80 after preincubation with Liproxstatin-1 (1 μM) or Deferiprone (100 μM) for 2 h and subsequent treatment with 25 μg/mL of $PM_{2.5}$ EI for 12 h

UNCORRECTED PROOF

using a lipid peroxidation assay kit. (**C**) Total iron levels are detected in HuTu-80 cells incubated with three types of PM after 12 h using an iron assay kit. (**D**) Total iron levels in HuTu-80 cells after preincubation with Liproxstatin-1 (1 μM) or Deferiprone (100 μM) for 2 h and subsequent treatment with 25 μg/mL of $PM_{2.5}$ EI for 12 h using an iron assay kit. (**E**) Western blot analysis after incubation of 25 μg/mL of three types of PM for 24 h. The experiment was repeated three times. *$p < 0.05$, #$p < 0.001$.

Figure 4. $PM_{2.5}$ with extraction ions induces ferroptosis by increasing ROS levels. (**A**) Detection of ROS in HuTu-80 cells in response to three types of PM after 24 h using 7′–dichlorofluorescin diacetate (DCFDA) fluorescence staining detected by flow cytometry. (**B**) Cell viability analysis after preincubation with N-acetylcysteine (NAC; 5 mM), mito-TEMPO (10 μM), or diphenyleneiodonium chloride (50 nM) for 2 h and subsequent treatment of 25 μg/mL of $PM_{2.5}$ EI after 24 h using WST-8. (**C**) Detection of ROS in HuTu-80 cells in response to 25 μg/mL of $PM_{2.5}$ EI for 24 h after preincubation with NAC (5 mM) or mito-TEMPO (10 μM) for 2 h using DCFDA fluorescence staining detected by flow cytometry. (**D**) Western blot analysis after incubation of 25 μg/mL of three types of PM for 24 h. (**E**) Detection of ROS in HuTu-80 cells in response to 25 μg/mL of $PM_{2.5}$ EI for 24 h after preincubation with liproxstatin-1 (1 μM) for 2 h using DCFDA fluorescence staining detected by flow cytometry. (**F, G**) Western blot analysis after preincubation with liproxstatin-1 (1 μM) or deferiprone (100 μM) for 2 h and subsequent treatment with 25 μg/mL of $PM_{2.5}$ EI for 24 h. The experiment was repeated three times. *$p < 0.05$, #$p < 0.001$.

UNCORRECTED PROOF

REFERENCES

1. Brunekreef B and Holgate ST (2002) Air pollution and health. Lancet 360(9341), 1233-1242
2. Cheng H, Gong W, Wang Z et al (2014) Ionic composition of submicron particles (PM1.0) during the long-lasting haze period in January 2013 in Wuhan, central China. J Environ Sci 26, 810-817
3. Frey A, Ramaker K, Röckendorf N et al (2019) Fate and translocation of (nano) particulate matter in the gastrointestinal tract. Biol Responses Nanoscale Particles Springer, Cham, 281-327
4. Beamish LA, Osornio-Vargas AR, Wine E (2011) Air pollution: An environmental factor contributing to intestinal disease. J Crohn's Colitis 5, 279-286
5. Wang Y, Zhong Y, Liao J, Wang G (2021) $PM_{2.5}$-related cell death patterns. Int J Med Sci 18, 1024
6. Michael S, Montag M, Dott W (2013) Pro-inflammatory effects and oxidative stress in lung macrophages and epithelial cells induced by ambient particulate matter. Environ Pollut 183, 19-29
7. Su LJ, Zhang JH, Gomez H et al (2019) Reactive oxygen species-induced lipid peroxidation in apoptosis, autophagy, and ferroptosis. Oxid Med Cell Longev, 2019
8. Dixon SJ, Lemberg KM, Lamprecht MR et al (2012) Ferroptosis: an iron-dependent form of nonapoptotic cell death. Cell 149, 1060-1072
9. Xie Y, Hou W, Song X et al (2016) Ferroptosis: process and function. Cell Death Differ 23, 369-379
10. Chen X, Li J, Kang R, Klionsky DJ, Tang D (2021) Ferroptosis: machinery and regulation. Autophagy 17, 2054-2081

UNCORRECTED PROOF

11. Woodby B, Schiavone ML, Pambianchi E et al (2020) Particulate matter decreases intestinal barrier-associated proteins levels in 3D human intestinal model. Int J Environ Res Public Health 17, 3234

12. Conrad M, Kagan VE, Bayir H et al (2018) Regulation of lipid peroxidation and ferroptosis in diverse species. Genes Dev 32, 602-619

13. Wang Y and Tang M (2019) $PM_{2.5}$ induces ferroptosis in human endothelial cells through iron overload and redox imbalance. Environ Pollut 254, 112937

14. Kwon MY, Park EH, Lee SJ and Chung SW (2015) Heme oxygenase-1 accelerates erastin-induced ferroptotic cell death. Oncotarget 6, 24393-24403

15. Towers C G, Wodetzki D and Thorburn A (2020) Autophagy and cancer: Modulation of cell death pathways and cancer cell adaptations. Journal of Cell Biology 219

16. Liu Y, Zhao D, Peng W et al (2021) Atmospheric PM2.5 blocking up autophagic flux in HUVECs via inhibiting Sntaxin-17 and LAMP2. Ecotoxicology and Environmental Safety 208, 111450.

17. Charoud-Got J, Emma G, Seghers J et al (2017) Preparation of a $PM_{2.5}$-like reference material in sufficient quantities for accurate monitoring of anions and cations in fine atmospheric dust. Anal Bioanal Chem *409,* 7121–7131

UNCORRECTED PROOF

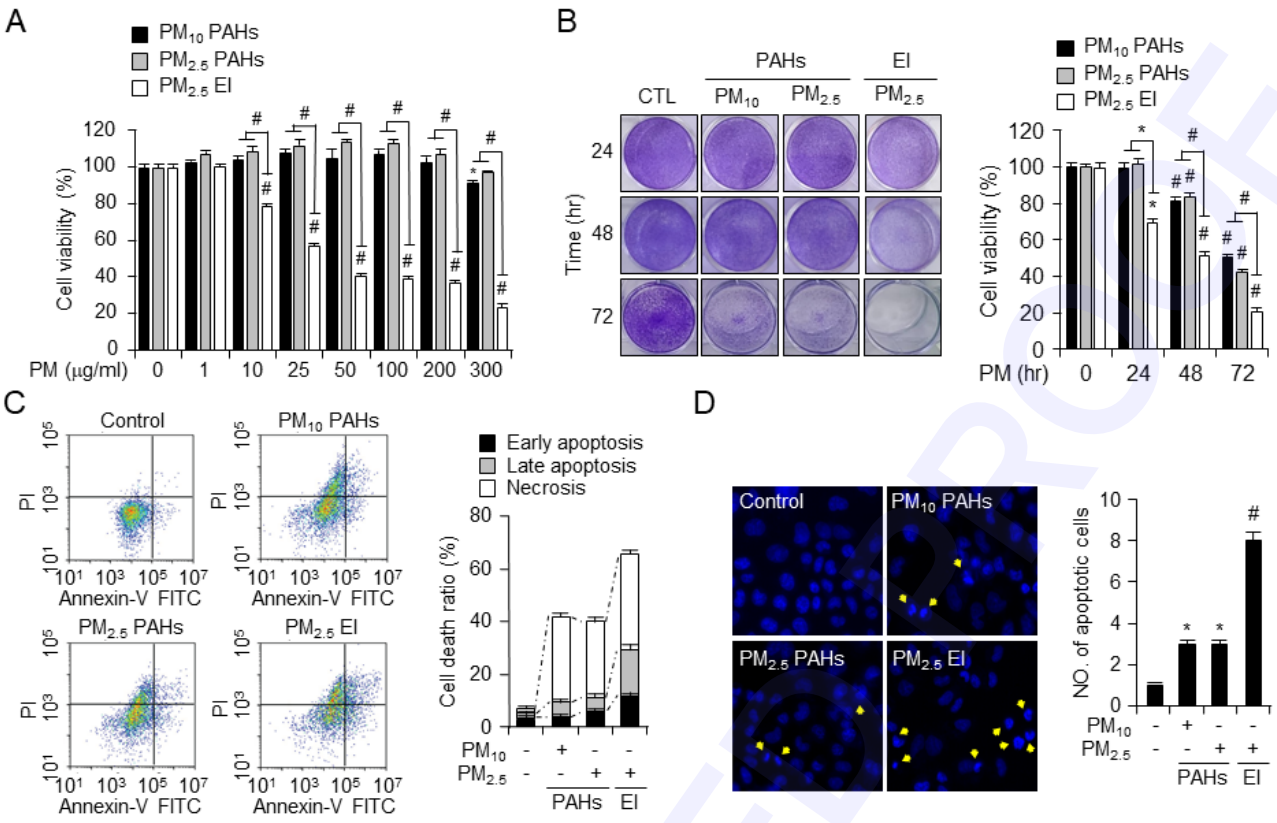

Figure 1

Fig. 1. Figure 1

UNCORRECTED PROOF

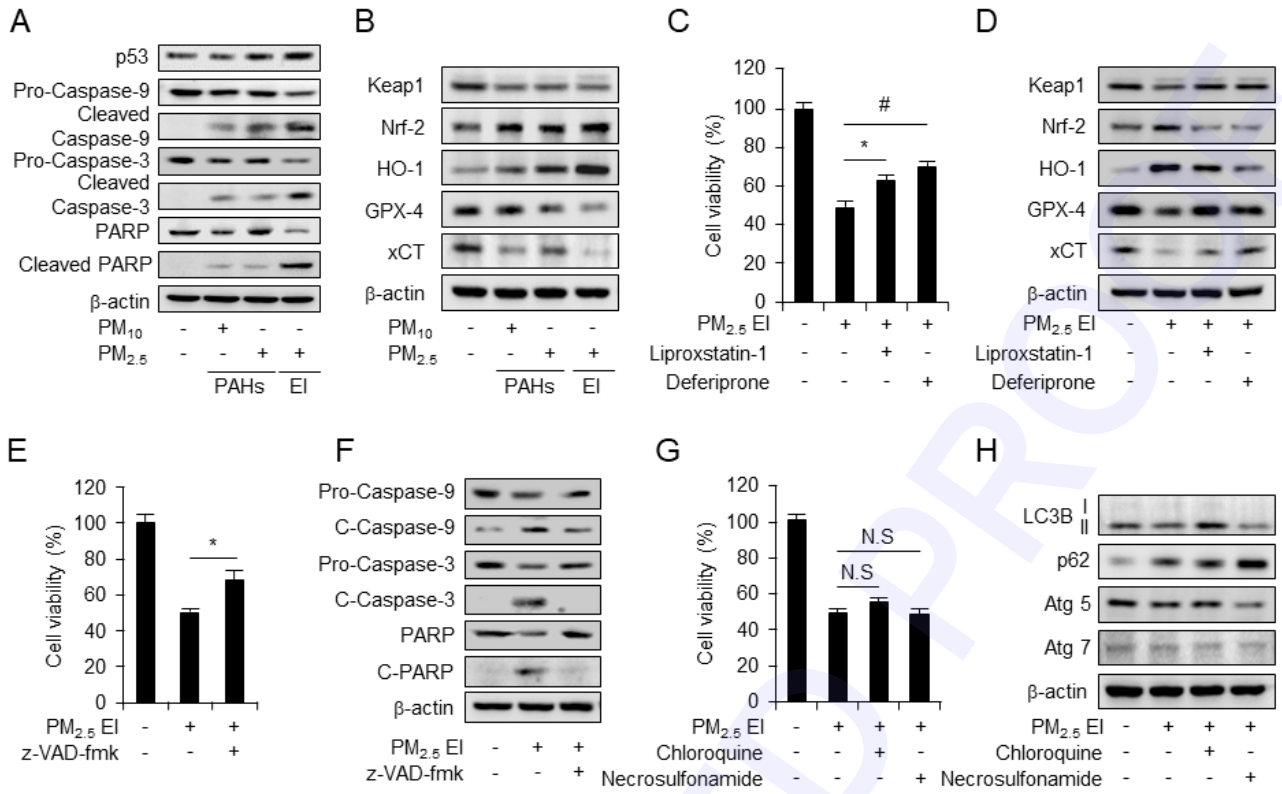

Figure 2

Fig. 2. Figure 2

UNCORRECTED PROOF

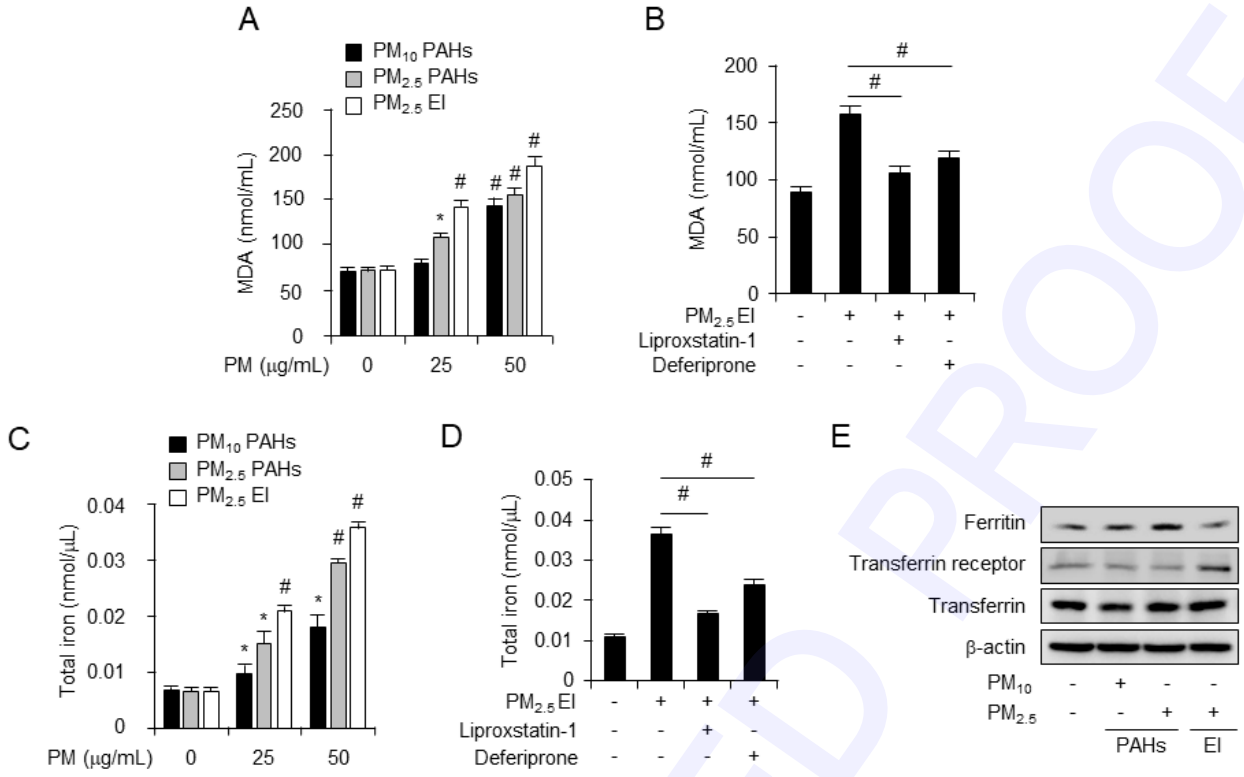

Figure 3

Fig. 3. Figure 3

UNCORRECTED PROOF

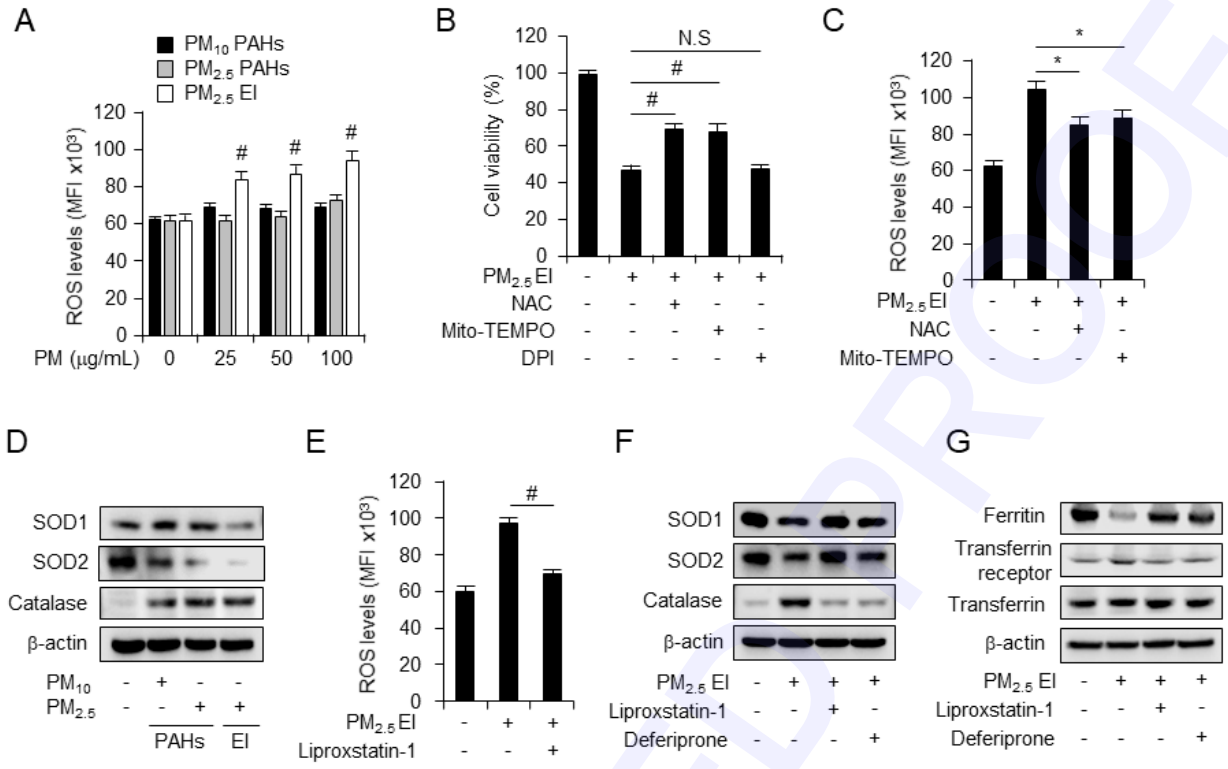

Figure 4

Fig. 4. Figure 4

UNCORRECTED PROOF